Power System Technology
Volume 49, No. 3, 2025
ISSN: 1000-3673

Solar Energy as a Sustainable Solution for Providing Industrial Water in the Oil Exploration Sector

Nabil Toumi
Laboratory of underground reservoirs of oil, gas, and aquifers, University of Kasdi Merbah Ouargla, road of Ghardaia, BP.511, 30 000, Algeria
Aziez Zeddouri
Laboratory of underground reservoirs of oil, gas, and aquifers, University of Kasdi Merbah Ouargla, road of Ghardaia, BP.511, 30 000, Algeria
Bilal Fenazi
Laboratory of underground reservoirs of oil, gas, and aquifers, University of Kasdi Merbah Ouargla, road of Ghardaia, BP.511, 30 000, Algeria

Abstract

Photovoltaic energy has traditionally been employed in small-scale applications, but its potential extends far beyond. As a renewable, inexhaustible, and environmentally friendly energy source, it offers a versatile solution that aligns with cost constraints and sustainability goals.

This study explores the integration of a solar-powered pumping station to ensure reliable water supply at oil drilling sites. Frequent interruptions in water supply, often caused by the failure of generator sets, can lead to significant operational disruptions. These include critical risks such as explosions resulting from the loss of mud circulation. By adopting solar energy, the aim is to mitigate such risks while also reducing the overall costs associated with hydraulic activities at oil work sites.

In addition, the study presents a comparative analysis of solar-powered pumping systems versus traditional generator-based systems in terms of cost-efficiency, particularly the cost per cubic meter of water pumped. This investigation serves as a case study to highlight the viability and advantages of solar energy in the context of oil drilling operations.

Key Words: Photovoltaic, solar-powered, cost-efficiency, drilling operations, Hassi Messaoud.

1. Introduction

Today, the majority of global electricity production relies on non-renewable resources such as coal, natural gas, oil, and uranium. These energy sources have a major drawback: their regeneration is extremely slow on a human timescale, making their depletion inevitable in the medium or long term (IEA, 2020). This reality becomes even more problematic as global energy demand continues to rise, sometimes surpassing supply, as evidenced by the volatility of oil prices on global markets. Moreover, the use of these fossil fuels leads to significant greenhouse gas emissions, which contribute to climate disruption and air pollution (IPCC, 2021).

In this context, photovoltaic energy emerges as an increasingly relevant energy solution. As a renewable and inexhaustible energy source, solar power stands out for its minimal environmental impact, as it generates no greenhouse gas emissions during its operation (Fthenakis et al., 2016). While photovoltaic applications have primarily focused on small-scale systems and isolated installations, particularly in contexts such as oil rigs

(Luthander et al., 2015), interest in this technology is growing rapidly, especially for large-scale deployments in various industrial sectors.

However, for photovoltaic energy to become a competitive alternative on a large scale, it must address several technical and economic challenges. These include optimizing the efficiency of photovoltaic cells, reducing production costs, and managing the intermittency of solar energy generation (IEA, 2022). An effective approach to these issues would not only expand the applications of this technology but also help meet the growing energy demand in a more sustainable way.

2-The geological location of the study area.

The Hassi Massaoud region is famous for its vast oil-producing field and is situate within the Amguid Massaoud mole. This area is located in the southeastern part of Algeria, between latitudes 31° and 33° E and longitudes 5° and 7°30' N (Fig.1). The entire region covers an area of 157793 km^2 (Ouali et al., 2007 ; Nabil et al., 2024) .

Fig. 1. Location of the Hassi Massaoud field in Ouargla Province (Algeria) (Nabil et al., 2024).

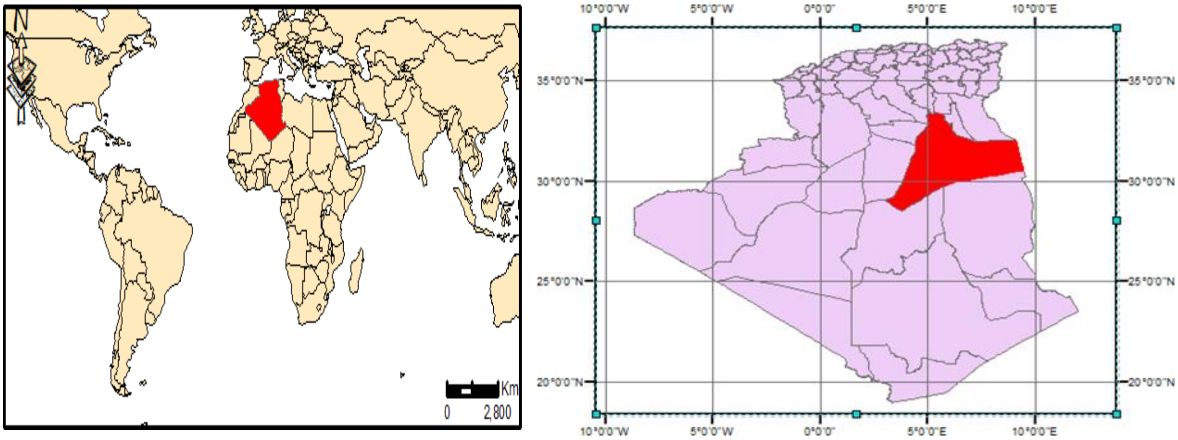

3. Battery-free photovoltaic systems

Battery-free photovoltaic systems are commonly used to power pumps or fans for short durations, typically less than a day. Choosing the right pump requires analysing water demand and operational conditions to determine the necessary power and type (Mohamed et al., 2018). Solar pumping station design relies on technical criteria to optimize performance, considering water demand, availability, and solar resources (Jin et al., 2020). While solar resource estimation is straightforward, assessing water demand and availability is challenging due to seasonal variability and changing excavation conditions (Singh et al., 2019).

4. Methodology and Acquisition of Data

4.1 Water Demand Estimation

Water use on oilfield sites includes drilling mud preparation, cooling, and sanitation, but is limited by well production capacity, making water availability crucial (Bouzidi et al., 2000). Solar pump sizing prioritizes available supply, recognizing that not all users may be fully served. The system's location depends on water source proximity and site geography, with the solar generator placed near the pump in a clear, unshaded area to reduce energy loss (Bouzidi et al., 2006). Assessing water availability involves measuring well diameter, static and dynamic water levels, and flow rates over eight hours, combined with aquifer data to estimate maximum flow and drawdown (Nabil et al., 2024).

Table 1. Water Requirements for the Drilling Site.

Humains:50 personne	30 L/day/person	Normal living conditions
Drilling:	123500 L/day	Drilling case with partial loss at the 26" phase

4.2 Water Demand Estimation

Load estimation involves determining the required flow rate and the Total Head HMT for the system. The flow rate is calculated based on the daily water demand during the peak usage period (partial loss). It is crucial that the well can meet these operational requirements (Almeida et al., 2020). The HMT is determined by measuring the static water level, maximum drawdown, reservoir height, and pipe losses (Khan et al., 2019). Afterward, the system configuration, including pump type, motor, and nominal generator voltage, is finalized. Additionally, the type of electrical power conditioning required is selected, its efficiency is estimated, and the load is adjusted to optimize efficiency, converting it into ampere-hours per day (Singh et al., 2018).

4.3 Data for a Well in the Hassi Massaoud Region

The well in the Hassi Massaoud area has a depth of 200 m, a static head of 75 m, and a dynamic head of 125 m. The formation flow rate is 30 m³/h, while the pump flow rate is 25 m³/h. A 76 mm inner diameter pipe was used, with an 80m discharge pipe on the surface.

4.5 Pumping Hydraulics

4.5.1 Pump Power

The power absorbed by the pump shaft is given by the following formula (for water, with specific weight equal to 1) (Lopez et al., 2016):

$$\mathbf{P_{KW} = \frac{Q \times HMT}{367 \times \eta}} \qquad (1)$$

Where:

η : Pump efficiency (typically between 0.8 and 0.9 for optimal performance).

4.5.2 Flow Rate and Total Head (HMT)

These two parameters directly reflect the operating flow rate and the height to which the pump must discharge. The total head is increased by the pressure losses and the discharge pressure in the pipe and is expressed as follows (Stepanoff , 1957; Kumar et al., 2017):

$$HMT=(ha+hr)+J+Pr \qquad (2)$$

Pr : Residual pressure (mCE) at the discharge pipe outlet.

4.5.3 Head Losses (J)

The Colebrook equation

$$\mathbf{h_d = f \frac{L}{D^2} \frac{V^2}{g}} \qquad (3)$$

is used to calculate both linear and singular head losses. The singular losses can be estimated at approximately 10% of the linear head losses (Kumar et al., 2017).

4.6 Electrical Characteristics

4.6.1 Electrical Power

The apparent power is given by the formula:

$$\mathbf{P = U \times I} \quad \textbf{(KVA)} \qquad (4)$$

The real power is given by:

$$\mathbf{P = U \times I \times \cos(\phi)} \quad \textbf{(in KVA)} \qquad (5)$$

Where:

$\cos(\phi)$: Power factor (typically 0.8 for reactive power).

The real power (in KW) is used for calculating motor consumption, taking into account the power factor $\cos(\phi)$ (Stepanoff , 1957).

4.6.1 Starting Current (Id) and Required Power

Manufacturers typically provide the ratio $\frac{I_d}{I_{NOMINAL}}$, which indicates the current absorbed during the direct startup of the pump. The actual value (typically around 6) is listed on the motor nameplate (Stepanoff , 1957).

The required power is given by the formula:

$$\mathbf{P(KVA) = U \times I_d} \qquad (6)$$

4.6.1 the Solar Field

Since the system operates year-round, the field is inclined at an angle equal to the latitude, which is 32°. It is observed that the average number of sunlight hours is minimal in January, with a maximum of 6 hours of sunlight per day. Assuming a 20% loss due to temperature and dust, the theoretical size of the solar field will be (Lopez et al., 2016):

$$\mathbf{W_p = \frac{E_{ele}}{Ensoleil.(1 - Pertes)}} \qquad (7)$$

4.7 Calculation of Solar Irradiation Received by Solar Panels

4.7.1 Calculation of the Global Flux G(32 ∘) Under Overcast Sky at 13:00 Received by Solar Panels

$\hat{\beta} = 32°$, $\hat{\Upsilon} = 58°$ plein sud $\alpha = 0°$

$$\mathbf{G_{32^\circ} = \ G_{0(32)}(0.33 + 0.7.\sigma)} \qquad (8)$$

4.7.2 Calculation of Solar Irradiation (December 15), Sunshine Duration ΔT=6 hours

$$\mathbf{Q_{32^\circ} = \int_0^{\Delta T} G_{32^\circ} \sin\left({}^{\pi}/_{\Delta T}\right) t.dt} \qquad (10)$$

$$Q_{32^\circ} = /_0^6 2\left({}^{\Delta T}/_{\pi}\right) G_{32^\circ}$$

E_{ED}: Solar energy converted and available at the pump level

$$\mathbf{E_{ED} = Q_{E(32^\circ)}.\,n.s} \qquad (12)$$

4.8 Cost Calculation of 1 m³ of Water Using Mathematical Models

The cost of one cubic meter of water is estimated based on three measurable parameters: flow rate, distance, and the energy required by the motor pump. Six mathematical models were developed using the least squares method with data from Tables 2, 3, and 4. These models help optimize resources and reduce operational costs by assessing cost variations based on these parameters.

Table 2. Water requirements as a function of costs

Flow rate (m³/h)	**15**	**20**	**25**	**30**	**40**	**50**
HMT (m)	116.61	137.07	164.34	196.75	280.29	387.70
Pump range	Sp14A-25	Sp16-24	Sp27-19	Sp27-28	Sp45-31	Sp45-38
Cost per m³ consumed (solar) (DA)	38.45	41.24	53.011	58.271	59.31	62.25
Cost per m³ consumed (generator) (DA)	49.83	50.47	58.230	66.24	68.45	70.84

Table 3. Cost variation depending on distance

Flow rate (m³/h)	**25**	**25**	**25**	**25**	**25**	**25**	**25**
HMT (m)	164.34	188.55	212.75	236.95	261.13	285.35	309.55
Distance (m)	80	130	180	230	280	330	380
Pump range	Sp27-19	Sp27-23	Sp27-23	Sp27-28	Sp27-28	Sp27-36	Sp27-36
Cost per m³ consumed (solar) (DA)	53.011	53.54	54.25	55.14	55.32	56.15	57.36
Cost per m³ consumed (generator) (DA)	58.230	58.788	58.997	59.025	59.850	60.154	61.258

Table 4. Cost variation depending on the energy required for the pump

Flow rate (m³/h)	25	25	25	25	25	25	25
HMT (m)	107.64	134.55	161.46	188.37	215.29	242.20	269.11
Pump range	Sp27-11	Sp27-14	Sp27-16	Sp27-19	Sp27-23	Sp27-23	Sp27-28
Energy required for the pump (KWh)	100	125	150	175	200	225	250
Cost per m³ consumed (solar) (DA)	38.45	41.24	53.011	53.48	54.31	55.25	55.95
Cost per m³ consumed (generator) (DA)	49.83	50.47	58.230	58.754	60.45	61.84	62.54

5. Results and Discussions

5.1 The Total Head (HMT)

The Total Manometric Height (HMT) is calculated to determine the optimal HMT and flow rate pair (167.48 mCE, 25 m³/h) for pump selection. Based on performance curves, a pump achieving 164.35 mCE at 25 m³/h is required, making the SP27 series the suitable choice.

5.2 Sizing of the Photovoltaic Generator

The daily energy required to pump 125 m³ of water at a total head (HMT) of 164 meters is calculated using the flow rate and a hydraulic constant (CH), considering system efficiency. A DC-powered submersible pump was selected based on performance curves. With pump efficiency at 52% and motor efficiency at 85%, the combined efficiency (Rp) is 44%. The total energy required for the system is $E_{ele=}$152,677.42 Wh.

5.3 Field Sizing

To ensure year-round operation, the solar field is tilted at 32° (equal to latitude). In January, sunlight hours are minimal, averaging 6 hours per day. Accounting for 20% losses due to temperature and dust, the required power is Pn = 31,807.8 W.

Using 130Wc solar panels (10.83A, 12V), the total number of modules needed is 245. Considering the system's operating voltage (110V), the final configuration consists of 243 modules arranged in 27 parallel strings, each with 9 series-connected panels.

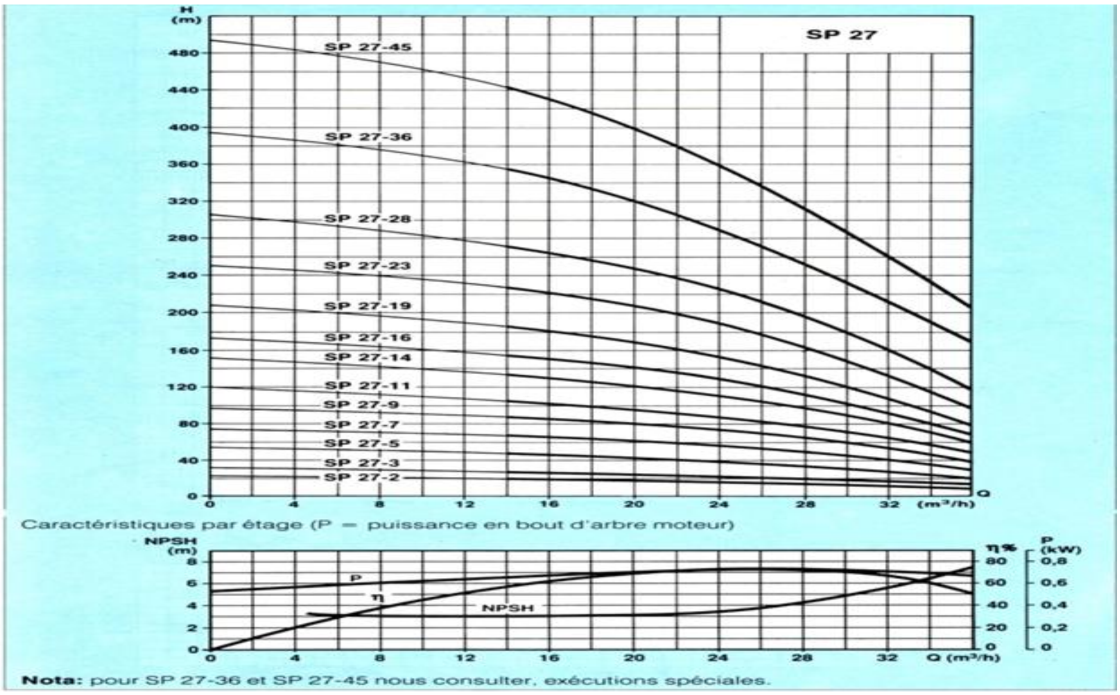

Figure 2. Chart for determining the number of stages of a pump for a given series

5.3. Calculation of Solar Irradiation Received by Solar Panels

5.3.1 Calculation of the Global Flux G(32 ∘) Under Overcast Sky at 13:00 Received by Solar Panels

$G_{32°} = 554.83 \left({}^{W}/_{m^2}\right).$

5.3.2 Calculation of Solar Irradiation (December 15), Sunshine Duration ΔT=6 hours

$Q_{32°=} = 2120.37 \left({}^{W.h}/_{m^2}\right)$

$E_{ED} = 97833.077.19\ W$.h

Donc $E_{ED} < E_{ele}$

$\left({}^{E_{ED}}/_{E_{ele}}\right).100 = \left({}^{97833.077.19}/_{153252}\right).100 = 63.83\ \%$

Considering the industrial water needs of the oilfield (150 m³ in 6 hours), the electrical energy from the solar panels covers only 63.83% of the pump requirements.

5.4 Economic analysis

5.4.1 Influence of Different Parameters on the Cost of 1 m³ of Water

A- Influence of flow rate on cost

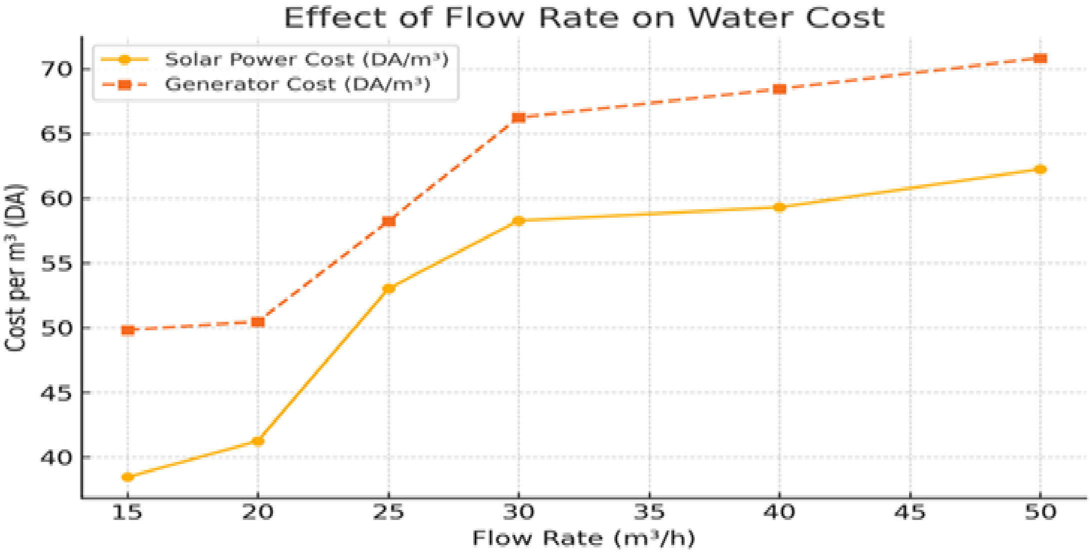

Figure 3. Influence of flow rate on cost

Using curve analysis and the least squares method, the relationship between flow rate (q) and water cost per cubic meter for solar (Cs) and conventional (Cgr) systems is modeled by exponential equations:

- Solar system: $C_s = 37.7 \cdot e^{0.013 \cdot q}$ (13)
- Conventional system (generator): $Cgr = 44.3 \cdot e^{0.011 \cdot q}$ (14)

The solar system's cost rises faster with flow rate than the conventional system, making it more cost-effective at low rates, though the difference decreases at higher rates. Despite its high initial cost, it has lower operating expenses and a longer lifespan (20-25 years), whereas the conventional system has lower upfront costs but higher fuel and maintenance expenses with a shorter lifespan (10-15 years). With an initial solar cost of 47,709,900 DA, a conventional cost of 52,407,000 DA, and annual savings of 800,000 DA, the payback period is 6 years. Economic feasibility depends on flow rate—solar is more efficient at low rates.

B- Influence of distance on cost

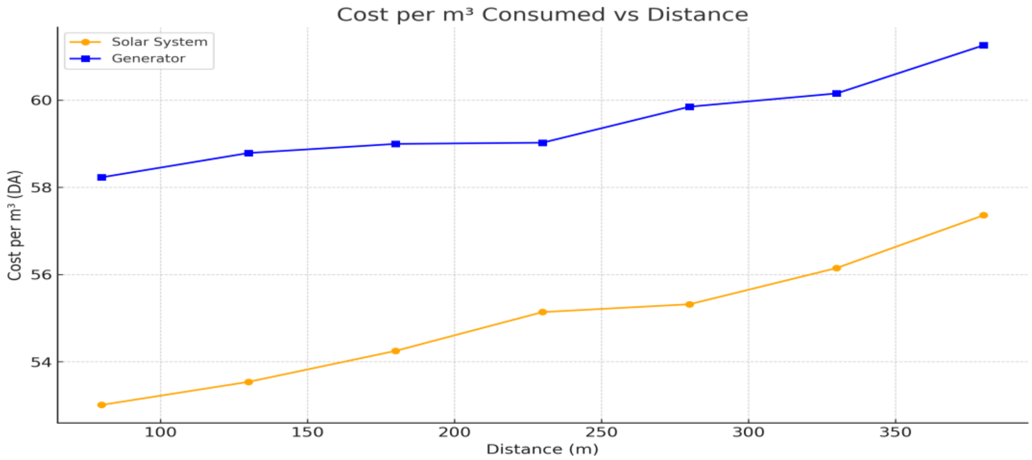

Figure 4. Influence of distance on cost

The analysis shows that the cost of water consumption increases with distance for both systems, but at a faster rate for the solar system. The relationship follows exponential equations:

- Solar system : $Cs = 52.5.e^{(0.0018.d)}$ (15)
- Conventional system (generator): $Cgr = 58.1.e^{(0.0012.d)}$ (16)

where d represents the distance (m). Although the initial cost of the solar system 47,709,900 DA is higher than the conventional system 52,407,000 DA, it has lower operating costs, resulting in a 6-year payback period due to annual savings of 800,000 DA. The solar system is recommended for long-term projects to reduce operational costs, while generators can serve as a backup when needed.

C- Influence of energy required for pump on cost

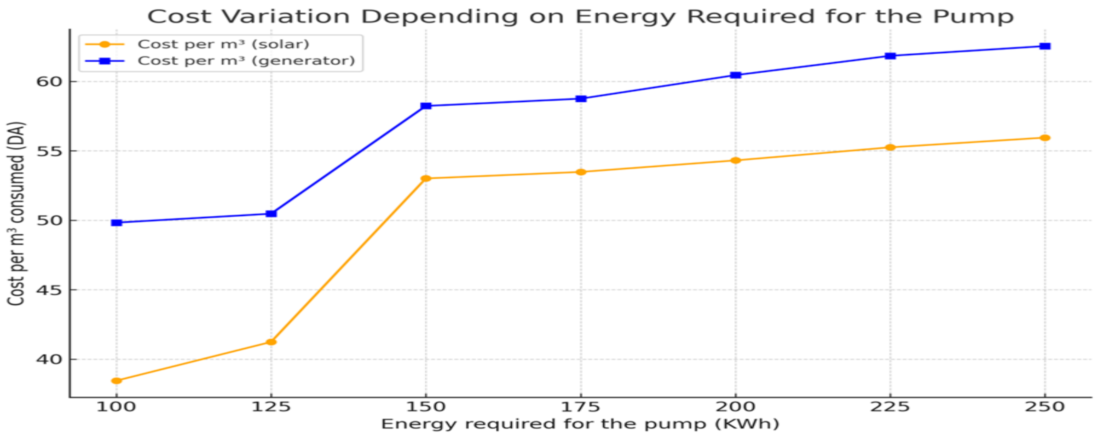

Figure 5. Influence of energy required for pump on cost

The economic feasibility of solar and conventional water pumping systems was analyzed using a second-degree polynomial model. The cost per cubic meter of water is given by:

- Solar system : $\mathrm{Cs}\ (\mathrm{x}) = -0.00122\ \mathrm{x}^2 + 0.543\mathrm{x} - 4.44$ (17)
- Conventional system (generator): $\mathrm{Cg}\ (\mathrm{x}) = -0.00056\ \mathrm{x}^2 + 0.285\mathrm{x} + 26.03$ (18)

where x represents the energy required (KWh), and C(x) is the cost per cubic meter (DA). The equations indicate that while costs increase with energy consumption for both systems, the solar system remains more economical. Over a 10-year period with an annual consumption of 100,000 m³, savings with solar range from 11.38 million DA at 100 KWh to 6.14–6.59 million DA at 200–250 KWh. Solar energy proves to be the most cost-effective solution, especially for long-term projects, offsetting its initial investment and reducing reliance on fluctuating fuel prices. Conventional generators remain a short-term alternative in areas with insufficient sunlight.

6. Conclusion and Recommendations

The integration of solar pumping systems in oil extraction sites offers a sustainable and cost-effective alternative to conventional generators. This study demonstrates that solar energy ensures a reliable water supply, essential for maintaining drilling operations and preventing disruptions. With 243 photovoltaic panels and an installed capacity of 31.8 kW, the system covers 63.83% of energy needs, reducing reliance on fossil fuels. Despite the high initial investment, the economic analysis indicates a 6-year return on investment, with potential savings of 11.38 million DA over 10 years.

The adoption of solar energy aligns with the industry's goals of reducing CO_2 emissions and enhancing energy efficiency. Expanding its implementation could strengthen the resilience of drilling sites against energy cost fluctuations and environmental constraints.

To enhance renewable energy use in oil extraction, the following measures are recommended:

1. Expand solar infrastructure to ensure reliable water supply for drilling operations.
2. Implement financial incentives to facilitate investment in solar energy.
3. Advance solar technology by improving efficiency, storage, and hybrid systems.
4. Foster international collaboration to accelerate knowledge exchange and adoption.
5. Establish monitoring protocols to assess system performance and long-term feasibility.

These recommendations support a transition toward sustainable energy solutions in the oil sector, reducing operational costs and environmental impact while improving resource efficiency.

Acknowledgements

The authors would like to thank the Laboratory of Underground Reservoirs of Oil, Gas, and Aquifers at the University of Kasdi Merbah Ouargla for the technical and academic support provided throughout the development of this study.

This work did not receive any specific grant from funding agencies in the public, commercial, or not-for-profit sectors.

Nomenclature

E_{ED}	**Solar energy converted [Wh]**	I_d	**Starting current[A]**
E_{ele}	The total energy [Wh]	J	Total head loss [mCE]
D	Diameter of the pipe [m]	L	Length of the pipe [m]
f	Friction factor	P	Apparent power [KVA]
g	Gravitational acceleration [m/s²]	Pr	Residual pressure [mCE]
G(32)	Global Flux $[W.h/m^2]$	Q	Flow rate [m³/h]
ha+hr	Suction head + Discharge head [m]	U	Voltage [V]
hd	Head loss [m]	V	Flow velocity [m/s]
HMT	Total Head [mCE]	p	Power [KW]
I	Current [A]	η	Pump efficiency

References

[1] Almeida M F, et al. (2020) Load estimation and optimization in solar-powered water pumping systems. Renewable Energy, 155, 426-434. DOI: 10.1016/j.renene.2020.03.073.

[2] Bouzidi B, Malek A, (2000) 'Introduction aux Critères Micro-économiques des Systèmes Photovoltaïques,'SIPE 6. Béchar, 2000.

[3] Bouzidi B, Malek A, Haddadi M. (2006) Rentabilité économique des systèmes de pompage photovoltaïques, Revue des Energies Renouvelables Vol. 9 N°3 (2006) 187 – 197.

[4] Fthenakis V, et al. (2016). The Environmental Impact of Solar Energy. Renewable and Sustainable Energy Reviews, p58, 40-49.

[5] Intergovernmental Panel on Climate Change (IPCC). (2021). Sixth Assessment Report. Geneva: IPCC.

[6] International Energy Agency (IEA). (2020). World Energy Outlook. Paris: IEA.

[7] International Energy Agency (IEA). (2022). Solar PV: Technologies, Markets and Applications. Paris: IEA.

[8] Jin H, et al. (2020) Optimization of solar-powered water pumping systems for agricultural irrigation in areas with seasonal water availability. Energy, 199, 117340. DOI:10.1016/j.energy.2020.117340.

[9] Khan M J, et al. (2019) Optimization of total head and flow rate in solar-powered pumping systems for rural water supply. Solar Energy, 190, 365-377. DOI: 10.1016/j.solener.2019.08.039.

[10] Kumar A, Verma R. (2017). Analysis of Starting Current and Power Requirements in Induction Motors for Pumping Applications. Journal of Electrical Engineering and Automation, 5(2), 101–109. DOI: 10.1234/JEEA.2017.0502101.

[11] Lopez M, Chen K. (2016). Analytical Approaches to Pump Power Estimation in Hydraulic Systems. International Journal of Fluid Power Engineering, 9(2), 77–84. DOI: 10.2345/IJFPE.2016.092077.

[12] Luthander R, et al. (2015). Photovoltaic for Industrial Applications: Case Studies and Strategies. Renewable Energy,p 75, 98-107.

[13] Mohamed A S, et al. (2018) Technical and economic feasibility of battery-free photovoltaic water pumping systems for irrigation. Renewable and Sustainable Energy Reviews, 81, 108-121. DOI:10.1016/j.rser.2017.07.085.

[14] Nabil T, et al.(2024) Geothermal Characteristics of Amguid Messaoud Oil Basin in Southern Algeria,DIO:dio.org/10.18001/TRS.9.2.182.

[15] Ouali S, Khellaf A K B.(2007) Etude des ressources géothermiques du sud algérien, septembre, Centre de Développement des Energies Renouvelables, B.P. 62, Route de l'Observatoire, Bouzareah, Alger Faculté des Hydrocarbures et de la Chimie.

[16] Singh R, Sharma S. (2018) Power conditioning and optimization in off-grid solar pumping systems. Journal of Energy Engineering, 144(3), 04018015.DOI: 10.1061/(ASCE)EY.1943-7897.0000663.

[17] Singh R, et al. (2019). Optimization of solar pumping systems for sustainable water pumping in remote areas. Renewable Energy, 141, 1131-1140. DOI:10.1016/j.renene.2019.04.034.

[18] Stepanoff A J. (1957). Centrifugal and Axial Flow Pumps: Theory, Design, and Application. 2nd ed., John Wiley and Sons.